DOI: 10.1007/s11099-013-0035-0 PHOTOSYNTHETICA 51 (3): 387-394, 2013

Effects of ectopically expressed hyperthermophilic archaeon (*Pyrococcus furiosus*) ribulose-1,5-bisphosphate carboxylase/oxygenase on tobacco photosynthesis

X.-G. LI[*,#,+], J. YANG[**,#], R. WANG[**], X.-F. TANG[***], J.-J. MENG[*], H.-J. QIN[****], X. LIU[****], F. GUO[*], and S.-B. WAN[*,+]

High-Tech Research Center, Shandong Academy of Agricultural Sciences and Shandong Provincial Key Laboratory of Genetic Improvement, Ecology and Physiology of Crops, Ji'nan, 250100, China[*]
Zhengzhou Tobacco Research Institute of China, National Tobacco Corporation, Zhengzhou, 450001, China[**]
College of Life Sciences, Wuhan University, Wuhan, 430212, China[***]
The State Key Laboratory of Plant Cell and Chromosome Engineering, Institute of Genetics and Developmental Biology, Chinese Academy of Sciences, Beijing, 100101, China[****]

Abstract

Pyrococcus furiosus is a hyperthermophilic archaeon. Its ribulose-1,5-bisphosphate carboxylase/oxygenase (PfRubisco) has only large subunit (L). PfRubisco has a novel $(L_2)_5$, decameric structure and it possesses higher carboxylase activity and thermotolerance. To assess the potential functionality of PfRubisco in higher plants under high-temperature stress, *PfRubisco* coding sequence was transiently expressed in *Nicotiana benthamiana* by *Pea early browning virus*-mediated ectopic expression. The transgenic *PfRubisco* plants produced chlorotic yellow stripes in their leaves. Relative to the control leaves, those with yellow stripes exhibited decreased net photosynthetic rate and chlorophyll content, altered chloroplast ultrastructure, and more severe photoinhibition of both photosystem I and II. We concluded that the ectopic expression of *PfRubisco* might disrupt the chloroplast development and function in *N. benthamiana*. The potential cause of the disruption was discussed.

Additional key words: high-temperature stress; *Nicotiana benthamiana*; photosynthesis; Rubisco; virus-mediated ectopic expression.

Introduction

Photosynthesis is one of the most sensitive biological processes that are negatively affected by higher temperatures (Quinn and Williams 1985, Salvucci and Crafts-Brandner 2004a,b). The optimum temperature range for photosynthesis for most C_3 plants falls between 20 and 35ºC and, in many cases, the peak rate of CO_2 assimilation and net photosynthetic rate (P_N) occurs well below 30ºC (Kumar *et al*. 2009). For higher plants, sensitivity of photosynthesis to higher temperature is related to inactivation of ribulose-1,5-bisphosphate carboxylase/oxygenase (Rubisco) at high temperatures (Schlenker and Roberts 2009). The Calvin cycle consists of 13 enzymatic reactions, among which Rubisco-catalyzed reaction is the only one that fixes CO_2 (Watson and Tabita 1997). Besides the photosynthetic eukaryotic organisms, numerous prokaryotes also rely on the Calvin cycle for CO_2 fixation, and many have been shown at least to harbor Rubisco (Tabita 1995). Rubisco proteins with

Received 31 May 2012, *accepted* 17 January 2013.
[+]Corresponding authors; tel: 00-86-531-83179047, fax: 00-86-531-83178156, e-mail: lixinguo@tom.com
Abbreviations: Chl – chlorophyll; C_i – intercellular CO_2 concentration; CK – noninoculated plants as a control; F_m – maximum yield of chlorophyll fluorescence in dark adapted state; F_v – variable fluorescence; F_v/F_m – maximal photochemical efficiency of PSII; GFP – green fluorescent protein; g_s – stomatal conductance; L – large subunit; *NbTp* – *Nicotiana benthamiana* ribulose-1,5-bisphosphate carboxylase/oxygenase small subunit transit peptide gene; NPQ – nonphotochemical quenching; P_N – net photosynthetic rate; PS – photosystem; qRT-PCR – quantitative reverse transcription-polymerase chain reaction; *rbc*L – large subunit of ribulose-1,5-bisphosphate carboxylase/oxygenase; *rbc*S – small subunit of Rubisco; RT-PCR – reverse transcription-polymerase chain reaction; Rubisco – ribulose-1,5-bisphosphate carboxylase/oxygenase; RuBP – ribulose-1,5-bisphosphate; S – small subunit; T – inoculated, transgenic *PfRubisco* plants; VMEE – virus-mediated ectopic expression.
Acknowledgements: This research was supported by the Natural Science Foundation of Shandong Province (ZR2009DZ007, ZR2011CQ042) and the Project of Seed Industry in Shandong Province.
[#]These authors contributed equally to this work.

sequence similarity are classified into four forms, which have dissimilar subunits and structures with various specificities for CO_2 and O_2 in different species.

Form I of Rubisco from higher plants consists of two distinct subunits, a large (L) and a small (S) one. Two L subunits generate two catalytic centers per L_2 dimer, the quaternary structure is L_8S_8 (Atomi 2002). This type of enzyme is prone to high-temperature stress. When crops are exposed to high temperatures, Rubisco protein and its activation can decrease in some crops (Larcher 2003, Lobell and Field 2007, Schlenker and Roberts 2009). Thermophilic archaeon is a type of bacteria, which can grow and reproduce in high-temperature environments. Hyperthermophilic archaeon *Pyrococcus furiosus* is an autotrophic organism, and its optimal growth temperature is above 65°C, while the lowest growth temperature is above 40°C. The high stability and the specific activity of archaeon Rubisco (form III) (Ashida *et al*. 2008) might be an important factor that enables archaeon to survive at high temperatures. Form III of Rubisco from archaeon, which conserves key amino acid residues important in catalysis between form I and form III proteins (Finn and Tabita 2003), shows higher carboxylase activity than any previously characterized Rubisco (Ezaki *et al*. 1999, Atomi *et al*. 2001, Maeda *et al*. 2002, Finn and Tabita 2003), and it has a novel $(L_2)_5$ decameric structure (Kitano *et al*. 2001) contributing to enhancing thermotolerance of the enzyme (Maeda *et al*. 2002).

To improve organic, especially higher plant photosynthesis under stress environments, some foreign Rubiscos were attempted to substitute in higher plant chloroplasts. But all these previous studies did not show any positive results. For example, the form I *rbc*LS operons from the rhodophyte, *Galdieria sulphuraria*, and the diatom, *Phaeodactylum tricornutum*, were inserted into the plastid genome of tobacco with negative effects on leaf CO_2 assimilation and plant growth (Whitney *et al*. 2001). Replacement of the plastomic *rbc*L gene of tobacco with its homologs from sunflower or the cyanobacterium, *Synechococcus* PCC 6301, did not result in hybrid hexadecameric Rubiscos capable of supporting photosynthetic growth (Kanevski *et al.* 1999). When Rubisco in tobacco was replaced with the form II of Rubisco from the α-proteobacterium, *Rhodospirillum rubrum*, and simultaneously, tobacco *rbc*L was reversely inhibited, the tobacco-*R. rubrum* transformants could grow only with CO_2 enrichment (Whitney and Andrews 2001).

It is unknown, whether the form III of Rubisco could improve thermotolerance of high plants. The form III of Rubisco from *P. furiosus* has not been yet reported to be inserted and integrated successfully into the genome of higher plants. In the present work, the form III of Rubisco from hyperthermophilic archaeon, *P. furiosus*, was assessed in *N. benthamiana* by virus-mediated ectopic expression (VMEE), which is used to mediate the ectopic expression of a cloned coding sequence in plant cells (Brisson *et al*. 1984, An *et al*. 2010).

Materials and methods

Plant materials and stress treatment: *Nicotiana benthamiana* was used as the plant material in the experiments. Plants were grown at 25/20°C (day/night) under about 18-h photoperiod [300−400 μmol m^{-2} s^{-1} photon flux density (PDF)] in a greenhouse. Plants with 2−3 leaves were used for injecting experiments, and they were used for determination 2 weeks later. For fluorescence determination, leaf discs were floated on the water at 32°C under the irradiance of 1,000 μmol m^{-2} s^{-1} PFD with the adaxial side face up. For photosynthesis determination, the temperature and irradiance was ensured by a leaf chamber of a portable CO_2 analyzer *CIRAS-1* (*Hansatech*, England).

Vectors and plasmid construction: According to the sequence of *rbc*S of *Nicotiana silvestris*, *Rubisco* gene (GenBank: X01722.1), *rbc*S of *Nicotiana benthamiana* Rubisco transit peptide gene (*NbTp*) was cloned by using a forward primer 5′-CTATGGCTTCCTCAGTTC-3′ and a reverse primer 5′-CTGCATTGCACTCTTCCG-3′. *NbTp* cDNA consisted of 171 bp open reading frame encoding a 57 aa polypeptide. *NbTp* was inserted into a vector pJIT163-p35S-*hGFP* by using a forward primer 5′-CTCCATGGCTTCCTCAGTTCTTTC-3′ introducing a *Nco*I cloning site at the 5′ end and a reverse primer 5′-CTCCATGG GCATTGCACTCTTCCG-3′ introducing a *Nco*I cloning site at the 3′ end of the fragment, then constructed plasmid pJIT163-p35S-*NbTp-hGFP* was used for intracellular targeting experiments.

Vectors, pCAPE1 and pCAPE2, used in VMEE were obtained from Dao-Wen Wang, Chinese Academy of Sciences. *PfRubisco* (GenBank: AE009950.1) was offered by Xiao-Feng Tang, Wuhan University, China. The full length sequence of the *PfRubisco* cDNA consisted of 1263 bp open reading frame encoding a 420 aa polypeptide. The VMEE constructs were conducted based on the methods of Liu *et al.* (2002) and Ryu *et al*. (2004) (Fig. 1). *PfRubisco* cDNA was inserted into vector pCAPE2 by using a forward primer 5′-CTACGCGT ATGAAGGTTGAGTGGT-3′ introducing a *Mlu*I cloning site at the 5′ end and a reverse primer 5′-CTGTCGAC TTTAGGCTTTAGGTAG-3′ introducing a *Sal*I cloning site at the 3′ end of the fragment. Subsequently, *NbTp* gene was inserted into vector pCAPE2-p35S-*PfRubisco*

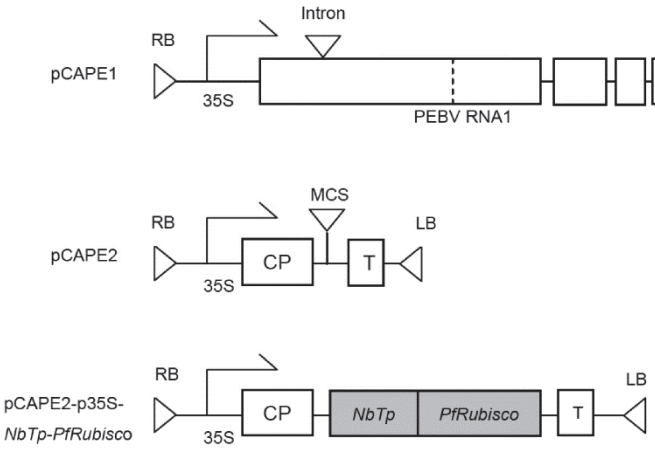

Fig. 1. Schema of pCAPE1 and 2 constructs: RB – right border, LB – left border, CP – coat protein, MCS – multiple cloning site, T – terminator.

to construct plasmid pCAPE2-p35S-*NbTp-PfRubisco* by using a forward primer 5′-CTCCATGGATGGCTTCCT CAGTTC-3′ introducing an *Nco*I cloning site at the 5′ end and a reverse primer 5′-CTACGCGTGCATTGCAC TCTTCCG-3′ introducing a *Mlu*I cloning site at the 3′ end of the fragment. Additionally, *NbTp* gene was inserted into vector pCAPE2 to construct plasmid pCAPE2-p35S-*NbTp* by using a forward primer 5′-CTCCATGGATGGCTTCCTCAGTTC-3′ introducing an *Nco*I cloning site at the 5′ end and a reverse primer 5′-CTACGCGTGCATTGCACTCTTCCG-3′ introducing a *Mlu*I cloning site at the 3′ end of the fragment.

VMEE: *Agrobacterium* strain GV3101 (Fig. 1) containing pCAPE1, pCAPE2-p35S-*NbTp*, and pCAPE2-p35S-*NbTp-PfRubisco* were grown in an incubator at 28°C on Luria-Bertani medium both with 10 μg L^{-1} rifampicin and 50 μg L^{-1} kanamycin for 2 d. Inoculum was prepared according to the protocol published previously (Ryu *et al*. 2004). Leaves of two weeks old *N. benthamiana* plants (with two or three leaves) were infiltrated with a 1:1 *Agrobacterium* mixture of either pCAPE1:pCAPE2-p35S-*NbTp-PfRubisco* or pCAPE1: pCAPE2-p35S-*NbTp*, respectively, as described earlier (Ryu *et al*. 2004). About 150 plants were infiltrated with *Agrobacterium* each time. After 2 weeks, more than 98% infiltrated plants showed yellow stripes on the leaf. Then, the fully expanded leaves of the plants with no inoculation (CK) and the inoculated plants (transgenic *PfRubisco* plants, T) with yellow stripes were used for experiments.

Intracellular targeting of putative NbTp-GFP: Green fluorescent protein (GFP) is a protein composed of 238 aa residues (26.9 kDa) that exhibits bright green fluorescence upon exposure to light in the blue to ultraviolet range. One DNA construct (pJIT163-p35S-*NbTp-hGFP*) was prepared to investigate the intracellular targeting of NbTp-GFP using transient expression in cowpea mesophyll protoplasts, which are usually used for intracellular targeting of exogenous gene by dual channel confocal microscopy, and this technology has been reported and accepted widely (Shah *et al*. 2002). The complete coding region of *NbTp* was subcloned into the pJIT163-p35S-*hGFP* vector, upstream and in frame with the *GFP* coding region. Cowpea mesophyll protoplasts were isolated, transfected with the above conduct (Shah *et al*. 2002), and examined by dual channel confocal microscopy (*FV500*, *IX70*, *Olympus*, Japan). The bright field image, GFP fluorescence and the red autofluorescence of chloroplast from protoplast expression were recorded simultaneously and compared. The potential colocalization of GFP fluorescence of chloroplast autofluorescence was further analyzed by checking the presence of yellow signals in the superimposed images.

Reverse Transcription-Polymerase Chain Reaction (RT-PCR): For the isolation of total RNA, leaf samples were pooled and homogenized under liquid nitrogen. Total RNA was isolated using Trizol (*Invitrogen*, USA) according to the manufacturer's instructions. About 30 μg total RNA were treated with RNase-free DNase. The RNA concentration and quality were assessed by photometric measurement (*Biophotometer*, *Eppendorf*, Germany) and gel electrophoresis. Approximately 3 μg total RNA was utilized to synthesize single stranded cDNA using reverse transcriptase (*SuperscriptIII*, *Invitrogen*, USA) and oligo-dT18 primers, according to the manufacturer's instructions.

Primers used to amplify 300 bp fragments of *PfRubisco* were: forward 5′-ATGAAGGTTGAGTGGTA-3′, reverse 5′-TTCATTCCGAAGATGT-3′; primers used to amplify 600 bp fragments of *PfRubisco* were as follows: forward 5′-ATGAAGGTTGAGTGGTA-3′, reverse 5′-ACGATAT CCCTAATCCT-3′; primers used to amplify 900 bp fragments of *PfRubisco* were as follows: forward 5′-ATGAAGGTTGAGTGGTA-3′, reverse 5′-TGATCAA CGCCAAT-3′; primers used to amplify the whole length (1263 bp) of *PfRubisco* were: forward 5′-ATGAAGGTTG AGTGGTA-3′, reverse 5′-TCATTTAGGCTTTAGGT-3′.

Quantitative RT-PCR (qRT-PCR): Single stranded cDNA was obtained according to the method of RT-PCR as mentioned above. Quantitative PCR was performed using SYBR green PCR master mix (*Takara*, Japan) in

optical 96-well reaction plates (*Applied Biosystems*, USA) on a mastercycler system (*Eppendorf*, Germany). The SYBR Green fluorescent dye was used to detect the synthesized dsDNA. A total reaction volume of 20 μl contained 10 μl Power SYBR Green Master Mix Reagent (*Applied Biosystems*, USA), 2 μl of diluted cDNA and 1 μl of each gene-specific primer (10 μM). PCR conditions were: 95°C for 2 min; 40 cycles of 95°C for 20 s, 55°C for 20 s, 72°C for 20 s, and then the melting curve. The data were expressed as the final cycle number necessary to reach a threshold fluorescence value (Ct). Data were normalized by the $2^{-\Delta Ct}$ method and 26S-RNA was used as a control housekeeping gene (Livak and Schmittgen 2001). At least three repeated trials were done in two independent biological replicates.

Primers of 26S-RNA used for Real-time PCR amplification for 300 bp fragments were as follows: forward 5′-GAAGAAGGTCCCAAGGGTTC-3′, reverse 5′-TCTC CCTTTAACACCAACGG-3′.

Primers of *N. benthamiana* Rubisco *rbc*L used for qRT-PCR amplification for 350 bp fragments were: *rbc*L forward 5′-AATCTTCTACTGGTACATGG-3′, reverse 5′-AGGTTTAATAGTACATCCCA-3′.

Chlorophyll (Chl) *a* fluorescence measurements: The maximal photochemical efficiency of photosystem (PS) II (F_v/F_m) expressed as the ratio of variable fluorescence (F_v) to maximum yield of fluorescence (F_m) was measured with a portable fluorometer (*FMS2*, *Hansatech*, King's Lynn, UK) according to the protocol described by Zhang *et al*. (2011). The initial fluorescence (F_0), which was measured by an analytical light of 6 nmol m^{-2} s^{-1} PFD, was recorded after a dark adaptation for more than 2 h, and subsequently a saturating pulse (6,000 μmol m^{-2} s^{-1} 6 μmol PFD, 0.6 s) was given to measure F_m.

The absorbance at 820 nm: The oxidizable P_{700} (P_{700}^+) was measured by the absorbance at 820 nm using a *Plant Efficiency Analyzer* (*Senior PEA*, *Hansatech*, King's Lynn, UK) described by Zhang *et al*. (2011). The first reliable measuring point for fluorescence change was at 20 μs, whereas the first measuring point for transmission change was at 400 μs. The time constant used for the transmission measurements was 100 μs. The light intensity used for the transmission measurements was 3,000 μmol m^{-2} s^{-1} PFD. The light was produced by four 650 nm LEDs (light-emitting diodes). The far-red source was a *QDDH73520 LED* (*Quantum Devices Inc*., Barneveld, WI, USA) filtered to 720 ± 5 nm. The modulated (33.3 kHz) far-red measuring light was provided by an *OD820 LED* (*Opto Diode Corp*., Newbury Park, CA, USA). Executing commands, such as turning on and off the LEDs, took approx. 250 μs. Turning on the red light and starting the measurement were synchronized commands. For the far-red light there was a delay of 250 μs between turning on the far-red light and the start of the measurement.

Chloroplast ultrastructure: The sample preparation and the electron microscope observation were done in electron microscope laboratory of the College of Life Sciences, Shandong Agricultural University. Pieces of leaves were fixed in 3.5% glutaric dialdehyde, washed in 0.1 mol L^{-1} PBS buffer, and then post-fixed in 1% perosmic acid, dehydrated through the gradient of ethyl alcohol, soaked, embedded, and polymerized in the Epon 812 resin. Then, embedded leaf samples were sliced using the *LKB-V* ultrathin slicer (*LKB*, Sweden) and double stained with the uranyl acetate and lead citrate. The observation, surveys, and photographs were conducted on the *JEM-1200EX* electron microscope (*JEOL*, Japan).

Gas-exchange: P_N was measured using a portable CO_2 analyzer *CIRAS-1* (*Hansatech*, England), stomatal conductance (g_s) and intercellular CO_2 concentration (C_i) were recorded simultaneously. The gas-exchange measurements were conducted at room temperature (25°C) and CO_2 concentration (390 μmol mol^{-1}) with the humidity of 45%, the air flow in the measuring chamber was 200 ml min^{-1}. P_N/PFD curves were measured with the measuring chamber under the temperature of 25°C. To measure the gas exchange at stress conditions, the chamber temperature was kept at 32°C, and the irradiance was 1,000 μmol m^{-2} s^{-1} PDF.

Chl: Pigments were extracted in 80% buffered acetone (25 mM Hepes, pH 7.5) and quantified spectrophotometrically using the extinction coefficients and wavelengths determined by Zhang *et al*. (2011).

Statistics: Data were analyzed using software *SPSS 16.0*, and *Duncan´s* multiple comparison tests were conducted between CK and T plants.

Results

Targeting of NbTp-GFP to chloroplast: To determine the subcellular localization of NbTp-GFP protein in plant cells, targeting experiments were performed *in vivo* in cowpea protoplasts derived from leaf tissue. In the protoplasts transformed with pJIT163-p35S-*NbTp-hGFP*, which expressed NbTp-GFP fusion cistron, the green fluorescence was clearly associated with chloroplasts and colocalized with the red autofluorescence of chloroplasts (Fig. 2). It showed that *N. tabacum* Rubisco small subunit transit peptide could locate an exogenous protein into chloroplast efficiently.

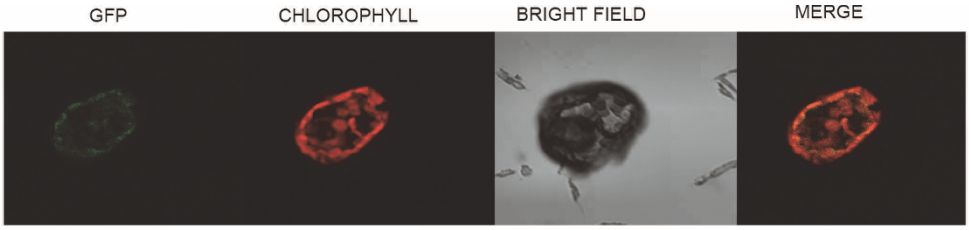

Fig. 2. Intracellular targeting of NbTp-GFP in cowpea protoplast. It shows cowpea protoplast transfected with p35S-*NbTp-GFP*, expressing NbTp-GFP fusion protein. Protoplasts were examined using dual channel confocal microscopy. Chloroplast targeting is demonstrated by colocalization of GFP fluorescence (*green*) and chloroplast (*red*), and the presence of chloroplast associated yellow signals due to superposition of the *green* (GFP) and *red* (chloroplast) fluorescence.

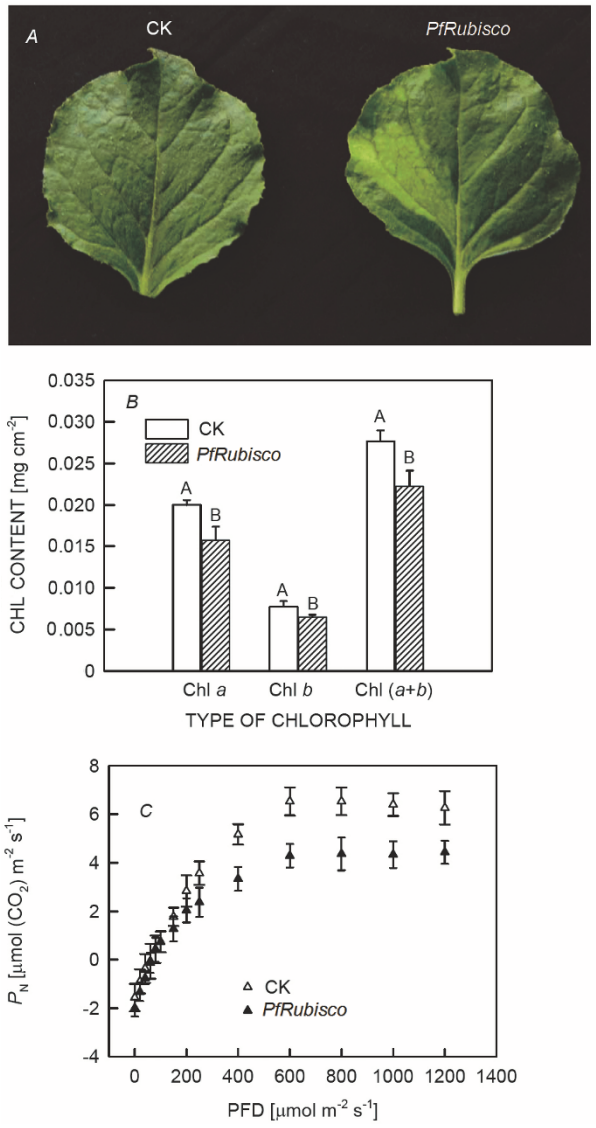

Fig. 3. Infection of *N. benthamiana* (*A*) and chlorophyll (Chl) content (*B*) and response curves of P_N to light (*C*). Each value was the average of three repeats of separate seedlings ± SD. *Different letters* in Fig. 3*B* indicate significant difference (P<0.05).

Phenotypes of transformed tobacco leaves: Leaves of T plants had a large area of yellow stripes relative to CK plants (Fig. 3*A*), nevertheless, the leaves of the plants inoculated with pCAPE2-*NbTp* had no colour changes in their leaves (data not shown). These results showed that yellow stripes were caused by the overexpression of *PfRubisco*. The contents of both Chl *a* and *b* in yellow stripes decreased obviously compared with those of CK plants (Fig. 3*B*). Simultaneously, photosynthetic light response curves showed difference between CK and T plants, the maximal P_N of transgenic plants was lower than that of CK plants (Fig. 3*C*).

Photosynthesis under high-temperature stress: Chl *a* fluorescence and absorbance at 820 nm were determined at 32°C and under 1,000 μmol m^{-2} s^{-1} PFD to assess the effect of PfRubisco on photosynthesis. During the stress, P_N of T plants decreased by about 85% (Fig. 4*A*); the decrease of P_N in the transgenic plants was accompanied by the decrease of g_s (Fig. 4*B*) and the increase of C_i (Fig. 4*C*). P_N, g_s, and C_i in CK plants showed no obvious change (Fig. 4*A*,*B*,*C*).

PSII in the leaves was estimated by measuring F_v/F_m. The ratio of F_v/F_m decreased in both CK and T plants during the stress, and it was affected more severe in the transgenic plants than in CK plants (Fig. 4*D*).

Photoinhibition of PSI is often estimated as P_{700}^+, which is measured as absorbance at 820 nm (Li *et al*. 2004, Zhang *et al*. 2011). When P_{700}^+ decreases, the peak value of absorbance at 820 nm decreases. Under the given growth conditions, P_{700}^+ of T plants was apparently lower than that of CK plants, it was only about 55.2% of CK plants (Fig. 4*E*). After 2-h stress, P_{700}^+ decreased by 52.7% in CK plants and by 74.8% in T plants, respectively (Fig. 4*E*).

Chloroplast ultrastructure in transformed tobacco leaves: Relative to CK plants, chloroplast development was apparently affected in T plants; the chloroplast number per cell was about 27.9 in CK and 12.7 in T plants, respectively (Fig. 5*A*). There were also some differences in chloroplast ultrastructure, higher grana stacks were found in T plants (Fig. 5*B*,*C*).

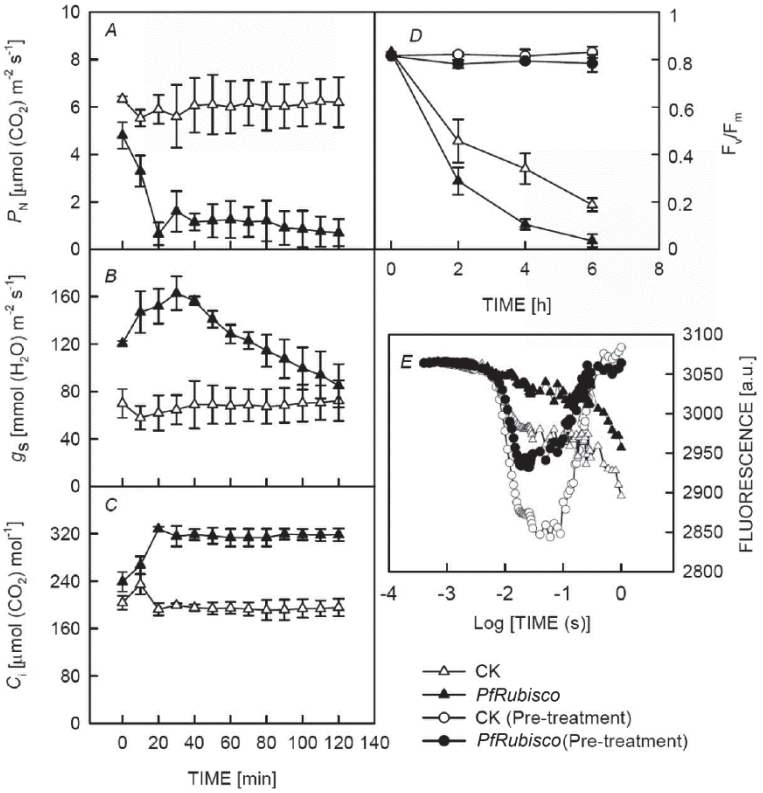

Fig. 4. Effects of stress at high temperature (32°C) under high irradiance [1,000 μmol m^{-2} s^{-1} PFD] on photosynthetic ability (*A*,*B*,*C*), F_v/F_m (*D*), and PSI reaction center activity (*E*) of inoculated plants. The data were determined during the treatment in *A*, *B*, *C,* and *D*, and the data were determined after the treatment in *E*. Each value for photosynthesis determination was the average of three repeats of separate seedlings during 2-h stress, and each value for PSI and PSII photoinhibition determination was the average of 15 repeats of separate seedlings during 6-h stress ± SD.

Effects of *PfRubisco* transformation on *N. benthamiana rbc*L expression: The nucleotide stretch of 100% identity was less than 10 nucleotides between *PfRubisco* and *N. benthamiana rbc*L, and it was higher than the identity between *PfRubisco* and *N. benthamiana rbc*S (data not shown). The expression of *N. benthamiana rbc*L detected by qRT-PCR in different positions of T leaves seemed not to be affected (Fig. 6*A*).

Additionally, only 300 bp, 600 bp, and 900 bp fragments of *PfRubisco* could be detected in the yellow stripes of T plant leaves and its full length could not be amplified by RT-PCR (Fig. 6*B*).

Discussion

The inactivation of Rubisco enzyme is usually one of the important factors related to the sensitivity of photosynthesis to higher temperature (Schlenker and Roberts 2009). Rubisco genes from thermotolerant species were attempted to be overexpressed in higher plants to improve their temperature resistance. There are some examples, such as *rbc*LS operons from the rhodophyte *G. sulphuraria* and the diatom *P. tricornutum* being transferred into tobacco (Whitney *et al*. 2001), replacement of the plastomic *rbc*L gene of tobacco with homologs from sunflower or the cyanobacterium, *Synechococcus* PCC 6301 (Kanevski *et al.* 1999), and replacement of tobacco Rubisco with Rubisco from the α-proteobacterium, *R. rubrum* (Whitney and Andrews 2001). Most of the above results were negative. All these failures were attributed to incompatibility between the plastid-encoded large subunits and the nucleus-encoded small subunits or by inability of the foreign Rubisco subunits to fold or assemble efficiently in the plastid (Whitney and Andrews 2001).

In the present work, *PfRubisco* coding sequence was expressed in tobacco by VMEE to assess the effects of PfRubisco on tobacco photosynthesis under high-temperature stress. Since NbTp could transit exogenous GFP protein into cowpea mesophyll chloroplast (Fig. 2), it was speculated that NbTp could help locate subunits of PfRubisco in tobacco chloroplast. Ectopical expression of *PfRubisco* induced the occurrence of yellow stripes in T plant leaves (Fig. 3*A*) and the decrease of the maximal P_N (Fig. 3*C*). The decrease of P_N in T plants was induced by nonstomatal limitation during the stress at high temperature under high irradiance (Fig. 4*A*,*B*,*C*) according to the assumptions of Farquhar and Sharkey (1982). More severe photoinhibition of PSII and PSI in T leaves relative to that in CK leaves (Fig. 4*D*,*E*) offered evidence that photosystem reaction centers were more sensitive to high temperature under high irradiance stress in T leaves than those in CK. It might be related to the lower Chl content (Fig. 3*B*), and the disturbed chloroplast development in T plants (Fig. 5), both of which induced the decline in photosynthesis (Fig. 3*C*). It was obvious that ectopical expression of *PfRubisco* coding sequence in tobacco by VMEE did not improve the resistance to high-temperature stress but it disturbed the chloroplast

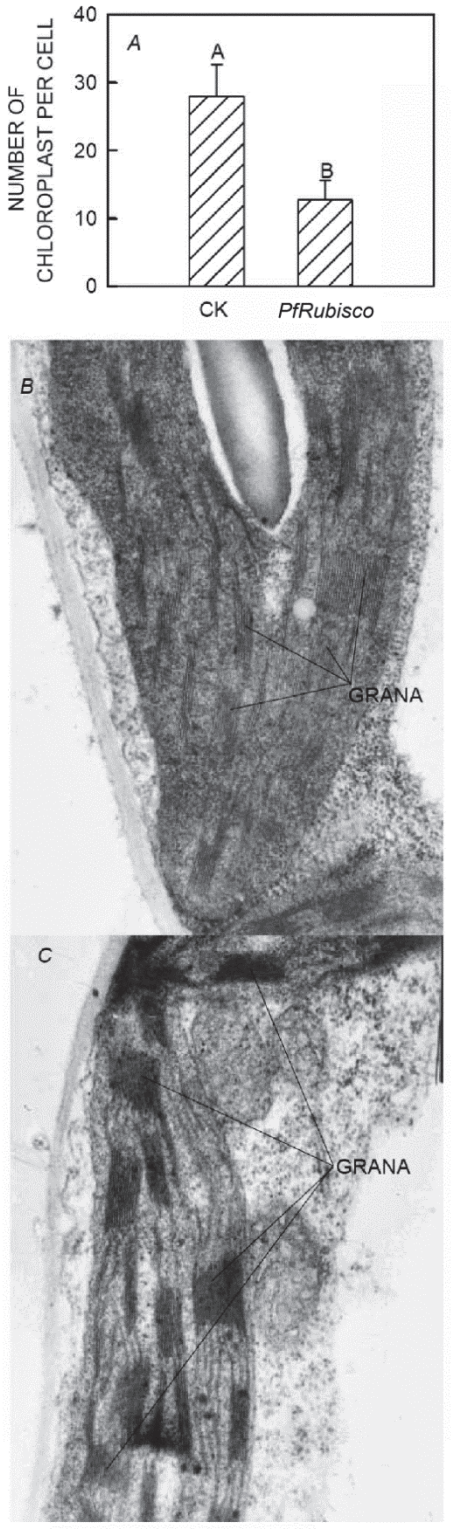

Fig. 5. Effects of expressing *PfRubisco* on tobacco chloroplast number (*A*) and its ultrastructure (*B* and *C*). Each value of (*A*) was the average of 25 cells from different leaves ± SD; (*B*) represents chloroplast from CK plants (2,500 ×); (*C*) represents chloroplast from T plants (2,500 ×). *Different letters* in *A* indicate significant difference (P<0.05).

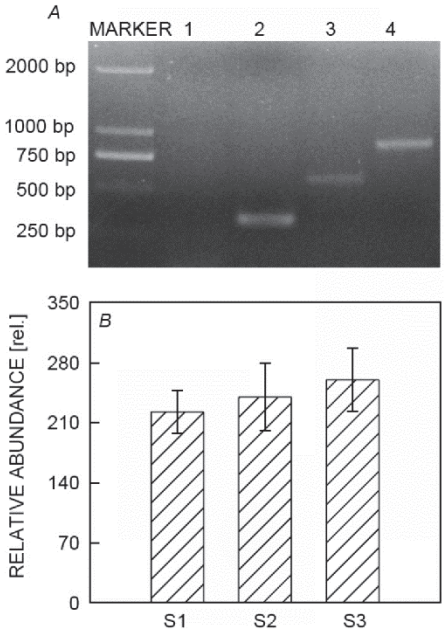

Fig. 6. RT-PCR of *PfRubisco* gene fragments in T plants (*A*) and relative expression levels of *N. benthamiana rbc*L gene (*B*). In Fig. 6*A*, lanes 1, 2, 3, and 4 represent 0−1,263 bp, 0−300 bp, 0−600 bp, and 0−900 bp of *PfRubisco* gene fragments of yellow stripes, respectively. In Fig. 6*B*, S1, S2 and S3 represent yellow stripes of T leaves (S1), green area of T leaves (S2) and CK leaves (S3). Data were means ± SD from independent biological replicates with three repeated trials, respectively.

development and reduced Chl content. According to previous reports concerning the exogenous *Rubisco* gene overexpression in higher plants, there were several possibilities. First, *PfRubisco* gene could be transcripted and translated, but its subunits could not recombine. Second, expression of *PfRubisco* gene disturbed intrinsic biological processes, *e.g.* the expression of NbRubisco subunits, Chl synthesis, grana lamellae organization. Third, *PfRubisco* gene could not be transcripted in *N. benthamiana*.

Heterologous gene sequences from both closely and distantly related plant species can be used to trigger the gene silencing in model plants as long as there is a minimal nucleotide sequence homology between the gene sequences (Ekengren *et al*. 2003, Ryu *et al*. 2004, Senthil-Kumar and Udayakumar 2006). The gene silencing can occur even with less than 21-nucleotide stretch of 100% identity between the trigger and target sequences (Senthil-Kumar *et al*. 2007). However, it seemed that the endogenous gene silence of *rbc*L of *N. benthamiana* was not induced by heterologous *PfRubisco* gene (Fig. 6*A*). From the results of RT-PCR shown in Fig. 6*B*, it was surprising that the full length of *PfRubisco* gene could not be detected in leaves of T plants. It was speculated that the incomplete transcription of *PfRubisco* gene might be related to the phenotype of T leaves, but this requires a further study.

References

An, X., Yu, C., Wang, D.: Assessment of plant gene functions using viral vectors. – In: Wang, A. (ed.): Principles and Practice of Advanced Technology in Plant Virology. Pp. 311-330. Kerala, India 2010.

Ashida, H., Saito, Y., Nakano, T. *et al.*: RuBisCO-like proteins as the enolase enzyme in the methionine salvage pathway: functional and evolutionary relationships between RuBisCO-like proteins and photosynthetic RuBisCO. – J. Exp. Bot. **59**: 1543-1554, 2008.

Atomi, H.: Microbial enzymes involved in carbon dioxide fixation. – J. Biosci. Bioeng. **94**: 497-505, 2002.

Atomi, H., Ezaki, S., Imanaka, T.: Ribulose-1,5-bisphosphate carboxylase/oxygenase from *Thermococcus kodakaraensis* KODl. – Methods Enzymol. **331**: 353-365, 2001.

Brisson, N., Paszkowski, J., Penswick, J.R. *et al.*: Expression of a bacterial gene in plants by using a viral vector. – Nature **310**: 511-514, 1984.

Ekengren, S.K., Liu, Y., Schiff, M. *et al.*: Two MAPK cascades, NPR1, and TGA transcription factors play a role in Pto-mediated disease resistance in tomato. – Plant J. **36**: 905-917, 2003.

Ezaki, S., Maeda, N., Kishimoto, T. *et al.*: Presence of a structurally novel type ribulose-bisphosphate carboxylase/oxygenase in the hyperthermophilic archaeon, *Pyrococcus kodakaraensis* KOD1. – J. Biol. Chem. **274**: 5078-5082, 1999.

Farquhar, G.D., Sharkey, T.D.: Stomatal conductance and photosynthesis. – Ann. Rev. Plant Physiol. **33**: 317-345, 1982.

Finn, M.W., Tabita, F.R.: Synthesis of catalytically active form III ribulose 1,5-bisphosphate carboxylase/oxygenase in archaea. – J. Bacteriol. **185**: 3049-3059, 2003.

Kanevski, I., Maliga, P., Rhoades, D.F., Gutteridge, S.: Plastome engineering of ribulose-1,5-bisphosphate carboxylase/oxygenase in tobacco to form a sunflower large subunit and tobacco small subunit hybrid. – Plant Physiol. **119**: 133-141, 1999.

Kitano, K., Maeda, N., Fukui, T., Atomi, H., Imanaka, T., Miki, K.: Crystal structure of a novel-type archaeal Rubisco with pentagonal symmetry. – Structure **9**: 473-481, 2001.

Kumar, A., Li, C., Portis Jr., A.R.: *Arabidopsis thaliana* expressing a thermostable chimeric Rubisco activase exhibits enhanced growth and higher rates of photosynthesis at moderately high temperatures. – Photosynth. Res. **100**: 143-153, 2009.

Larcher, W.: Physiological Plant Ecology, 4th Ed. Springer-Verlag, Berlin, 2003.

Li, X.G., Duan, W., Meng, Q.W. *et al.*: The function of chloroplastic NAD(P)H dehydrogenase in tobacco during chilling stress under low irradiance. – Plant Cell Physiol. **45**: 103-108, 2004.

Liu, Y., Schiff, M., Dinesh-Kumar, S.P.: Virus-induced gene silencing in tomato. – Plant J. **31**: 777-786, 2002.

Livak, K.J., Schmittgen, T.D.: Analysis of relative gene expression data using real-time quantitative PCR and the $2^{-\Delta\Delta C_T}$ method. – Method. **25**: 402-408, 2001.

Lobell, D.B., Field, C.B.: Global scale climate–crop yield relationships and the impacts of recent warming. – Environ. Res. Lett. **2**: 014002. doi:10.1088/1748-9326/2/1/014002, 2007.

Maeda, N., Kanai, T., Atomi, H., Imanaka, T.: The unique pentagonal structure of an archaeal Rubisco is essential for its high thermostability. – J. Biol. Chem. **277**: 31656-31662, 2002.

Quinn, P.J., Williams, W.P.: Environmentally induced changes in chloroplast membranes and their effects on photosynthetic function. – In: Barber, J., Baker, N.R. (ed.): Photosynthetic Mechanisms and the Environment. Pp. 1-47. Elsevier Science Publishers, Amsterdam 1985.

Ryu, C.M., Anand, A., Lang, L., Mysore, K.S.: Agrodrench: a novel and effective agroinoculation method for virus-induced gene silencing in roots and diverse *Solanaceous* species. – Plant J. **40**: 322-331, 2004.

Salvucci, M.E., Crafts-Brandner, S.J.: Relationship between the heat tolerance of photosynthesis and the thermal stability of Rubisco activase in plants from contrasting thermal environments. – Plant Physiol. **134**: 1460-1470, 2004a.

Salvucci, M.E., Crafts-Brandner, S.J.: Mechanism for deactivation of Rubisco under moderate heat stress. – Physiol. Plant. **122**: 513-519, 2004b.

Schlenker, W., Roberts, M.J.: Nonlinear temperature effects indicate severe damages to U.S. crop yields under climate change. – Proc. Natl. Acad. Sci. USA **106**: 15594-15598, 2009.

Senthil-Kumar, M., Hema, R., Anand, A. *et al.*: A systematic study to determine the extent of gene silencing in *Nicotiana benthamiana* and other *Solanaceae* species when heterologous gene sequences are used for virus-induced gene silencing. – New Phytol. **176**: 782-791, 2007.

Senthil-Kumar, M., Udayakumar, M.: High throughput virus-induced gene silencing approach to assess the functional relevance of a moisture stress-induced cDNA homologous to *Lea4*. – J. Exp. Bot. **57**: 2291-2302, 2006.

Shah, K., Russinova, E., Gadella Jr., T.W. *et al.*: The *Arabidopsis* kinase-associated protein phosphatase controls internalization of the somatic embryogenesis receptor kinase 1. – Gene Dev. **16**: 1707-1720, 2002.

Tabita, F.R.: The biochemistry and metabolic regulation of carbon metabolism and CO_2 fixation in purple bacteria. – In: Blankenship, R.E., Madigan, M.T., Bauer, C.E. (ed.): Anoxygenic Photosynthetic Bacteria. Pp. 885-914. Kluwer Academic Publishers, Dordrecht, The Netherlands 1995.

Watson, G.M.F., Tabita, F.R.: Microbial ribulose 1,5-bisphosphate carboxylase/oxygenase: a molecule for phylogenetic and enzymological investigation. – FEMS Microbiol. Lett. **146**: 13-22, 1997.

Whitney, S.M., Andrews, T.J.: Plastome-encoded bacterial ribulose-1,5-bisphosphate carboxylase/oxygenase (RubisCO) supports photosynthesis and growth in tobacco. – Proc. Natl. Acad. Sci. USA **98**: 14738-14743, 2001.

Whitney, S.M., Baldet, P., Hudson, G.S., Andrews, T.J.: Form I Rubiscos from non-green algae are expressed abundantly but not assembled in tobacco chloroplasts. – Plant J. **26**: 535-547, 2001.

Zhang, Y.J., Yang, J.S., Guo, S.J. *et al.*: Over-expression of the *Arabidopsis CBF1* gene improves resistance of tomato leaves to low temperature under low irradiance. – Plant Biol. **13**: 362-367, 2011.